FEM implementation of a viscoplastic model for calculating geomembrane strain due to differential settlement from degrading or thawing waste

4 authors:

Y. H. Fan
Queen's University
4 PUBLICATIONS **15** CITATIONS

SEE PROFILE

R. W. I. Brachman
Queen's University
123 PUBLICATIONS **2,746** CITATIONS

SEE PROFILE

Ronald Kerry Rowe
Queen's University
657 PUBLICATIONS **19,617** CITATIONS

SEE PROFILE

Hesham Eldesouky
Queen's University
9 PUBLICATIONS **79** CITATIONS

SEE PROFILE

Some of the authors of this publication are also working on these related projects:

Project   CO2 Seafloor Sequestration View project

Project   Field test regarding leaakge of cover GMBs View project

FEM implementation of a viscoplastic model for calculating geomembrane strain due to differential settlement from degrading or thawing waste

Y.H. Fan, R.W.I. Brachman, R.K. Rowe & H.M.G. Eldesouky
GeoEngineering Centre at Queen's–RMC-Queen's University,
Kingston Ontario, Canada

ABSTRACT

Geomembranes are widely used in landfill covers to control the infiltration of moisture and gas. Due to the degradation and consolidation of the underlying waste, it takes many years for the differential settlement to be complete. The differential settlement affects geomembrane strains during the process of degradation. For simplicity, in numerical calculations, the geomembrane is often assumed to be elastic. To investigate the implications of this assumption, a classical viscoplastic constitutive model for HDPE is implemented in the geometric nonlinear finite element analysis. The effect of the material properties and strain rates are investigated. Results based on the implementation of the viscoplastic model are compared with existing methods, showing the rate-dependent behaviour of HDPE should be considered when estimating the tensile strain in landfill covers that can develop due to differential settlement.

RÉSUMÉ

Les géomembranes sont largement utilisées dans les couvertures de décharge pour contrôler l'infiltration d'humidité et de gaz. En raison de la dégradation et de la consolidation des déchets sous-jacents, il faut de nombreuses années pour que le tassement différentiel soit complet. Le tassement différentiel affecte les déformations en tension des géomembranes au cours du processus de dégradation. Par souci de simplicité, dans les calculs numériques, la géomembrane est souvent supposée élastique. Pour étudier les implications de cette hypothèse, un modèle constitutif viscoplastique classique pour le PEHD est implémenté dans l'analyse par éléments finis géométriques non linéaires. L'effet des propriétés du matériau et des taux de déformation est étudié. Les résultats basés sur la mise en œuvre du modèle viscoplastique sont comparés aux méthodes existantes, montrant que le comportement dépendant de la vitesse du PEHD doit être pris en compte lors de l'estimation de la contrainte de traction dans les couvertures de décharge qui peut se développer en raison du tassement différentiel.

1 INTRODUCTION

Landfill covers are essential to control the infiltration of moisture and migration of gas from the waste (Rowe et al. 2004). A geomembrane is a critical element in a cover system intended to minimize fluid migration. However, due to the long-term degradation and thawing of frozen waste, the development of differential settlement results in strain and stress in geomembrane cover, making geomembrane susceptible to stress cracking and threatening the effectiveness of the barrier system.

Some researchers have analyzed the mechanical response of landfill liners (geomembrane), including strains and deformations. Rowe and Yu (2019) investigated the magnitude and significance of tensile strains in geomembrane landfill liners and discussed the experimental evidence of geomembrane cracking and failure when subject to excessive tensile strains.

One source of potential excess local geomembrane strains comes from liners used in the base of the landfill as there is significant overburden stress due to gravel used in a drainage system if there is not an adequate protection layer (Brachman and Eastman 2013, Eldesouky and Brachman 2018). This mechanism is less important for geomembranes in cover systems where the overburden stress is relatively low. However, geomembranes used in cover systems are even more susceptible to tensile strains

induced by differential settlement than those used in bottom liners. In particular, covers are susceptible to strains induced by differential settlement arising from both degradation of the waste and thawing of frozen waste.

Warith et al. (1994) monitored the rate of settlement and discovered that the settlement rate was essentially constant for the three years monitored following the completion of waste placement and construction of the final cover, without showing a decreasing trend. Yu and Bathurst (2017) studied the influence of soil and interface properties on numerical results of soil-geosynthetic interaction problems. Finley and Holtz (2001) performed a field investigation of landfills and related the geomembrane strain to surface settlement characteristics. Field experiments and numerical models were developed to calculate the strain in geosynthetic bridging sinkholes (Villard and Briançon 2008, Yu and Bathurst 2017). Considering the real size of landfills and interactions between different components, finite element analysis (FEA) was adopted to model the geometry of a full-scale problem, giving new insight regarding the importance of cover component properties (Eldesouky et al. 2020).

In most of these studies cited above, the geosynthetics were modelled as a linear elastic material with a single stiffness. However, generally speaking, geosynthetics are not elastic but rather rate-dependent materials (Bathurst and Naftchali 2021). With the rapid increase of computing

power of computer processors, finite element software is now capable of incorporating more sophisticated constitutive equations for geosynthetic components. Previous evaluations of a rate-dependent stiffness have included the development and validation of a viscoplastic constitutive model for HDPE pipes (Zhang and Moore 1997a, 1997b; 1997c). This experimental data was used in the validation of the constitutive model that captured the highly rate-dependent behaviour of the HDPE (Zhang and Moore 1997b). Ezzein et al. (2015) adopted a different approach and used a hyperbolic model for comparison with a general three-component model (Hirakawa et al. 2009) for modelling the rate-dependent behaviour of polypropylene reinforcement. In this context, a rate-dependent constitutive model for a cover geomembrane was implemented in a numerical analysis to evaluate the implications of the assumption of a linear elastic modulus for the geomembrane.

Because HDPE geomembranes are commonly used in cover systems, this paper implements the viscoplastic constitutive model for HDPE formulated by Zhang and Moore (1997c) in the finite element (FE) software ABAQUS (2017). The FE software is then used to predict the performance of cover geomembrane considering its rate-dependent behaviour. The results based on the current implementation are compared for the same problem with the results of a large displacement numerical analysis that assumed a linear elastic geomembrane (Eldesouky et al. 2020).

2 NUMERICAL MODELLING DETAILS

2.1 Viscoplastic model

The Zhang and Moore (1997c) viscoplastic model was implemented in a new subroutine programmed in FORTRAN that is not part of the ABAQUS material library. To validate the present FE implementation, simulated uniaxial tensile tests of type IV specimens were conducted at different strain rates and the experimental data (Zhang and Moore 1997a) was compared with simulated tests performed using FE model incorporating the new viscoplastic subroutine. The full geometry of the dog bone specimen was modelled in a plane stress analysis. The dimensions and boundary conditions simulated were according to ASTM D638 (Figure 1). True stress and true strain are adopted in this paper. Five strain rates ranging from 10^{-3} %/s to 10 %/s were simulated and showed good agreement (Figure 2). Considering the lower strain rate from the slow degradation of the waste in the field, the model predictions with strain rates ranging from 10^{-8} %/s to 10^{-4} %/s are also plotted in Figure 2, although there are no experimental data for these strain rates.

To better visualize the mechanical property of HDPE geomembrane, the tangent stiffnesses were calculated (Figure 3) based on the stress-strain relationship (Figure 2). The tangent stiffnesses are sensitive to both strain state and strain rate. The tangent stiffness reduced at a diminishing rate as the strain rate decreased. When the strain rate is lower than 10^{-9} %/s, the stiffness tended to approach a constant value (Figure 3). The differences

between the assumption of elastic behaviour and the actual stiffness have implications on the strain and stress developed in a geomembrane used in a cover system, as discussed later.
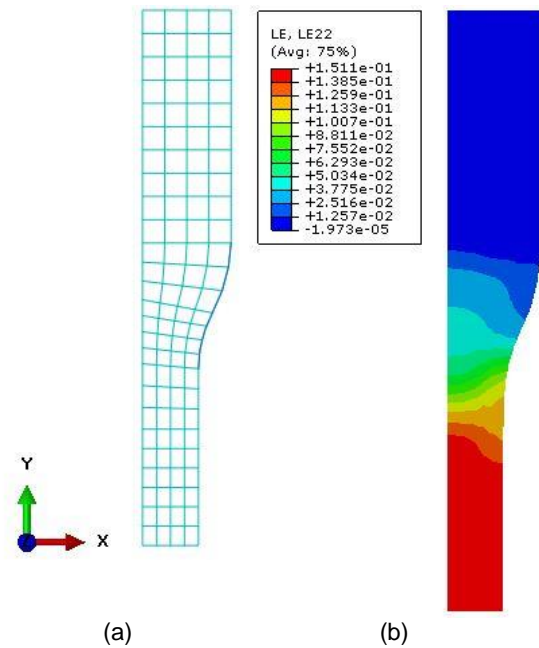
Figure 1. Finite element model of tensile test: (a) a quarter of type IV undeformed specimen with mesh (b) axial logarithmic (true) strain distribution in deformed shape

2.2 FINITE ELEMENT ANALYSIS

The objective of this study was to compare the results obtained assuming a linear elastic geomembrane with those obtained by modelling the geomembrane as viscoplastic material. Thus, except for the geomembrane constitutive model, exactly the same problem idealization (Figure 4) and finite element analysis were conducted as that reported by Eldesouky et al. (2020). The cover soil and waste were modelled as elastoplastic material with Mohr-Coulomb failure criterion. FEA model was discretized into 3400 elements with 10635 nodes to ensure accuracy. The properties of waste and soil are shown in Table 1 and Table 2. More details regarding this model are provided in Eldesouky et al. (2020).

The first procedure of the finite element analysis was a geostatic step in which the geostatic stress can reach equilibrium under gravity when the waste modulus is kept as 6 MPa. In the second procedure, the modulus of the entire waste dropped linearly to 0.7 MPa and the uniform settlement will occur. This step allowed the three parts of the model (waste, cover soil and cover geomembrane) to sufficiently contact each other and avoid potential convergence errors. In the first two procedures so far, the HDPE geomembrane was simplified to be linear elastic (E=1450 MPa) as the maximum strain of geomembrane is only 0.06 %. This simplification is reasonable because the stress was initially proportional to strain (Zhang and Moore 1997a). During the given time in the last procedure, the
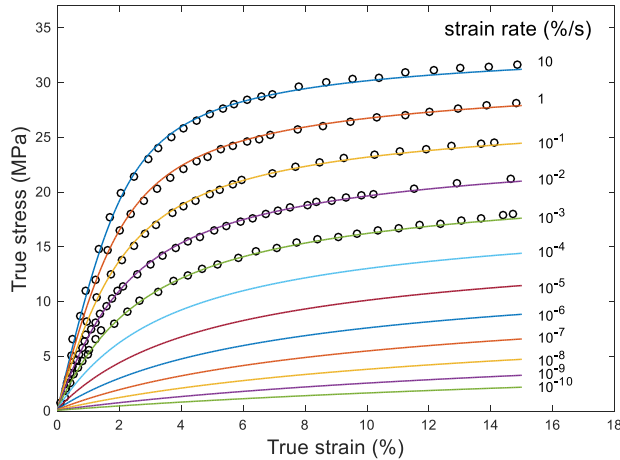
Figure 2. Experimental data for constant strain rate at 10^{-3} %/s to 10 %/s (Zhang and Moore 1997a) and model predictions for 10^{-8} %/s to 10 %/s
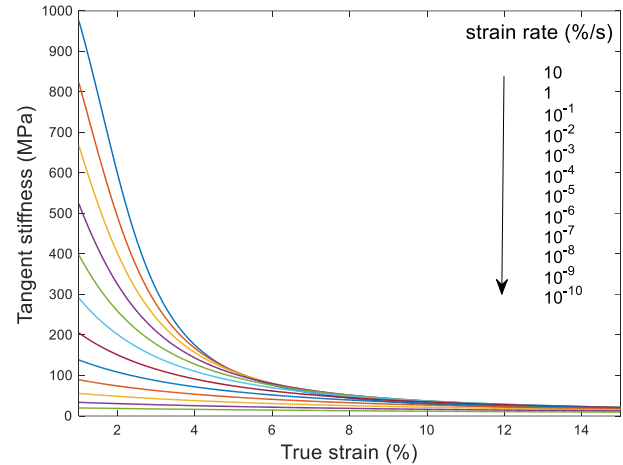
Figure 3. Stiffness of HDPE for rate at 10^{-10} %/s to 10 %/s
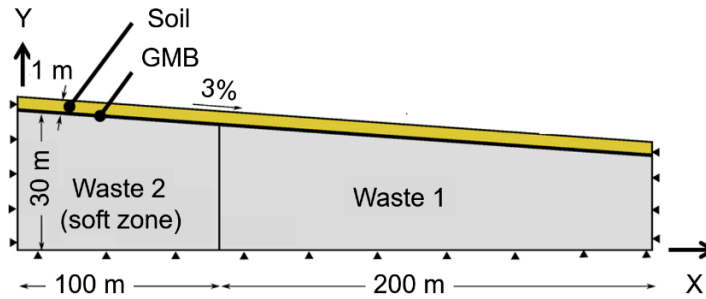
Figure 4. Schematic of the idealized finite element model

Table 1. Characteristics of the soil and waste

	Hard zone of Waste	Soft zone of waste	Cover soil
Stiffness E (MPa)	0.7	Variable (Table 2)	10
Poisson ratio	0.3	0.3	0.3
Cohesion (KPa)	25	25	1
Friction angle	25°	25°	25°

viscoplastic model subroutine started working, the stiffness of the soft zone (left part) decreased linearly from 0.7 MPa to 0.4 MPa over a prescribed period (discussed below). During this period, the settlement in the soft zone increased gradually and continuously. As a result, the geomembrane strain increased monotonically at a relatively constant strain rate. The length of the period over which differential settlement occurred was set to control the strain rate in the geomembrane and assess the effect of the rate of settlement on geomembrane performance.

3   RESULTS AND DISCUSSION

As the length of the degradation period increased, the stiffnesses of HDPE geomembrane decreased and became asymptotic to an approximately a constant value (around 30 MPa) (Figure 3). As a result, the case with a longer degradation period had a higher final maximum strain. For example, starting with an upper bound to the rate of deformation, a period of only 1-second was modelled to allow a full appreciation of the range over which the geomembranes rate-dependency affects the results (Case 1 in Table 2). In this case, a final maximum strain in the geomembrane of 8.4% was developed at an average strain rate of 8.4%/s. In Case 2, a time period for degradation of 3 years gave a higher final maximum geomembrane strain (11.2%) developed at an average strain rate of 10-7%/s. In contrast, if it took 30 years for the same level of degradation, the final maximum strain of geomembrane was 11.6% developed at an average strain rate of 1.2×10-8%/s (Case 3 in Table 2). The maximum strain in Case 3 was only 0.4% higher than that in Case 2 because the stiffnesses of both cases were very close to each other with the strain rate lower than 10-7 %/s (Figure 3). Therefore, a 3-year period corresponding to the strain rate of 10-7%/s in Case 2, was conservative enough for this finite element analysis. Case 2 was set as the base case for comparison later.

Case 4 was compared with Case 2 to investigate the implications of the assumption that geomembrane is linear elastic with a single stiffness of 150 MPa (Eldesouky et al.

Table 2. Model parameters in FEA model

case	Interface friction angle	Waste stiffness Soft zone (MPa)	Time period	Geomembrane property	Maximum Strain	Average strain rate (%/s)
1. Viscoplastic (VP) 1 s	20°	0.4	1 second	VP	8.4%	8.4
2. VP 3 years (base case)	20°	0.4	3 years	VP	11.2%	10^{-7}
3. VP 30 years	20°	0.4	30 years	VP	11.6%	1.2×10^{-8}
4. elastic	20°	0.4	-	150 MPa	9.6%	-
5. softer soft zone (VP)	20°	0.35	3 years	VP	18.7%	2.0×10^{-7}
6. softer soft zone (elastic)	20°	0.35	-	150 MPa	14.9%	-
7. smoother interface (VP)	5°	0.4	3 years	VP	11.0%	1.2×10^{-7}

2020). The results showed Case 4 (9.6% maximum strain) with an elastic geomembrane yielded a 1.6% lower strain than 11.2% obtained with the viscoplastic model in Case 2. Thus, a simplified single stiffness of 150 MPa underestimated the maximum geomembrane strain in a landfill cover system.

In Case 5, with the viscoplastic model, decreasing the stiffness of waste soft zone by one eighth increased the maximum strain to 18.7% or 1.7-fold higher than the base case value of 11.2% (Case 2). In contrast, with the linear elastic geomembrane, the same reduction of the stiffness of soft zone in Case 6 resulted in 1.5-fold higher maximum strain than Case 4. In short, the assumption of an elastic geomembrane underestimated the maximum strain more significantly with the larger differential settlement due to lower stiffness in the soft zone.

Case 7, in which a smooth geomembrane was compared with Case 2 textured geomembrane, showed that a smoother interface reduced the maximum strain by only 0.2 %. This is consistent with the conclusion drawn by Eldesouky et al. (2020).

The final strain distribution along the geomembrane showed compressive (negative) strains to the left of the shear surface (x=100m) and tensile (positive) strains to the right of the shear surface due to differential settlement (Figure 5). The magnitude of strains from Case 2 was higher than Case 3 and Case 4 all along the geomembrane. Because geomembrane failure usually arises from stress cracking related to tensile strain (Rowe and Yu 2019), the location of the maximum tensile strain in the geomembrane is the most critical location although stress cracking can be expected at any location where the strain exceeds about 4%. (e.g., see Figure 5 for Case 2).

The differential settlement δ in this context was defined as the difference in vertical movement between the two points located at soft zone and hard zone that exbibit the greatest relative movement (Figure 6). The relationship between the maximum strain developed and differential settlement δ is plotted in Figure 7. Three behavioural stages can be identified. In stage I (0 m ≤ δ ≤ 0.3 m), the strain barely changed because there was only uniform settlement in the geomembrane and constitutive model was irrelevant. In stage 2, the geomembrane strain increased essentially linearly with differential settlement and was dependent on the race of differential settlement, and hence the instituted model of the geomembrane. Coincidentally, in stage 2, the elastic analysis with E=150

MPa (Case 4) gave essentially the same relationship between strain and differential settlement as the viscoplastic analysis for Case 2 for 0.3 m ≤ δ ≤ 1.5 m. At δ~1.5m, the elastic analysis (Case 4) entered stage 3 and exhibited an increase in the rate of development of strain with differential settlement. Case 2 entered stage 3 at δ~2.2 m while Case 1 entered stage 3 at δ~2.6 m. The explanation for this is that the viscoplastic model of HDPE geomembrane yielded decreasing stiffness with higher strain (Figure 3).
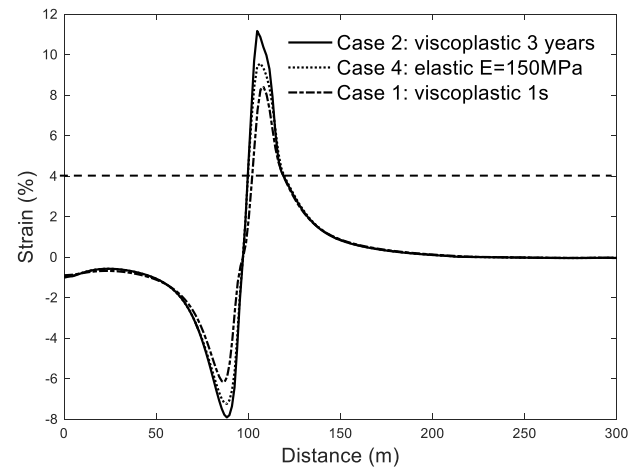
Figure 5. Geomembrane strain in x-direction

The final stresses inferred from different cases were more sensitive to strain rate than strain (Figure 8). Case 1, yielded over 4-fold higher stress than Case 2, showing the significance of choosing the reasonable time of degradation when modelling the stress in the geomembrane. The elastic analysis of Case 4 gave twice the maximum stress obtained from the viscoplastic Case 2.

Figure 6. Differential settlement δ
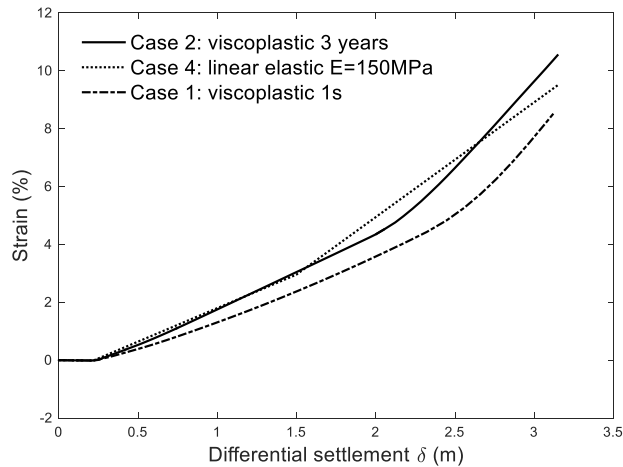
Figure 7. Development of geomembrane strain with differential settlement
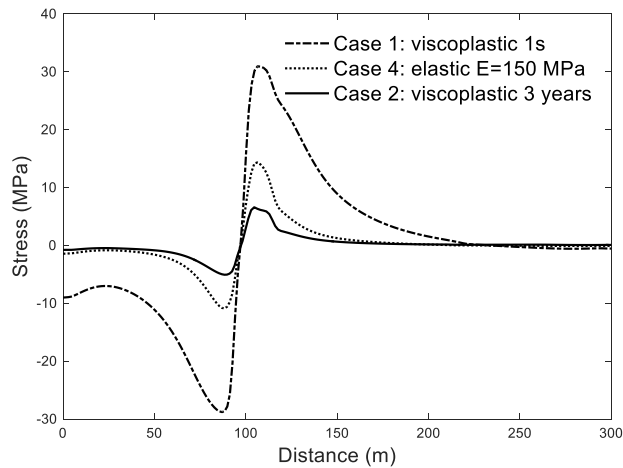
Figure 8. Geomembrane stress in x-direction

4   CONCLUSIONS

The implications of linear elastic assumption for geomembrane in a landfill cover system were investigated by implementing a time-dependent visco-plastic constitutive model into an idealized finite element analysis (Eldesouky et al. 2020). The modelling examined the strains and stresses developed in the geomembrane for a range of periods over which the differential settlement occurred ranging from 1s to 3 and 30 years. For the numerical analyses and parameters examined in this study, the following conclusions were reached:

1. With the viscoplastic model implemented for the geomembrane, the final maximum geomembrane strain increased with lower strain rates at a diminishing rate. When the strain rate decreased from 10^{-7} %/s to 1.2×10^{-8} %/s, the maximum strain only increased by 0.4%.
2. The simplified method with an assumption of a linear elastic modulus (150 MPa) for geomembrane underestimated the final maximum strain in geomembrane by 1.6% compared to the method with a viscoplastic model for geomembrane considering three years of gradual and continual settlement.
3. With the larger differential settlement due to lower stiffness in soft zone, modelling the geomembrane as an elastic material with the modulus of 150 MPa underestimated the maximum strain more significantly than the viscoplastic analysis because the stiffness of geomembrane decreased with strain in the viscoplastic model. This indicated that the implementation of the viscoplastic model becomes more necessary when more critical scenarios are considered.
4. The simplified method of linear elastic modulus (150 MPa) for geomembrane overestimated the final maximum stress of geomembrane (up to twice as much). Reasonable time should be considered because maximum stresses are more sensitive to strain rate than maximum strain.

5   ACKNOWLEDGEMENTS

6   REFERENCES

ABAQUS. 2017. Abaqus/CAE user manual. 2017. Dassault Systèmes, Providence, RI, USA.

ASTM D638. 2010. Standard Test Method for Tensile Properties of Plastics. ASTM International, West Conshohocken, PA, USA.

Bathurst, R. J., and Naftchali, F. M. 2021. Geosynthetic reinforcement stiffness for analytical and numerical modelling of reinforced soil structures, *Geotextiles and Geomembranes*, https://doi.org/10.1016/j.geotexmem.2021.01.003.

Brachman, R. W. I., and Eastman, M. K. 2013. Calculating local geomembrane indentation strains from measured radial and vertical displacements, *Geotextiles and Geomembranes*, 40: 58-68.

Eldesouky, H. M. G., and Brachman, R. W. I. 2018. Calculating local geomembrane strains from a single gravel particle with thin plate theory, *Geotextiles and Geomembranes*, 46(1): 101-110.

Eldesouky, H. M. G., Brachman, R. W. I., and Rowe, R. K. 2020. Factors affecting geomembrane strain from differential settlement, *GeoVirtual 2020*, The Canadian Geotechnical Society, Canada.

Ezzein, F. M., Bathurst, R. J., and Kongkitkul, W. 2015. Nonlinear load–strain modeling of polypropylene geogrids during constant rate‐of‐strain loading, *Polymer Engineering & Science*, 55(7): 1617-1627.

Finley, C. A., and Holtz, R. D. 2001. Investigation and modeling of two composite landfill covers, *Geosynthetics International*, 8(2): 97-112.

Hirakawa, D., Kongkitkul, W., Tatsuoka, F., and Uchimura, T. 2003. Time-dependent stress–strain behaviour due

to viscous properties of geogrid reinforcement, *Geosynthetics International*, 10(6): 176-199.

Rowe, R.K., Quigely, R.M., Brachman, R.W.I., and Booker, J.R. 2004. *Barrier Systems for Waste Disposal Facilities*. 2nd edition., CRC Press, Ontario, Canada.

Rowe, R. K., and Yu, Y. 2019. Magnitude and significance of tensile strains in geomembrane landfill liners, *Geotextiles and Geomembranes*, 47(3): 439-458.

Villard, P., and Briancon, L. A. U. R. E. N. T. 2008. Design of geosynthetic reinforcements for platforms subjected to localized sinkholes, *Canadian geotechnical journal*, 45(2): 196-209.

Warith, M.A., Smolkin, P.A., and Caldwell, J.G. 1994. Evaluation of an HDPE Geomembrane Landfill Cover Performance, *Geosynthetics International*, 1(2): 201–219.

Yu, Y., and Bathurst, R. J. 2017. Influence of selection of soil and interface properties on numerical results of two soil–geosynthetic interaction problems, *International Journal of Geomechanics*, ASCE, 17(6): 04016136.

Zhang, C., and Moore, I. D. 1997. Nonlinear mechanical response of high density polyethylene. Part I: Experimental investigation and model evaluation, *Polymer Engineering & Science*, 37(2): 404-413.

Zhang, C., and Moore, I. D. 1997. Nonlinear mechanical response of high density polyethylene. Part II: Uniaxial constitutive modeling, *Polymer Engineering & Science*, e37(2): 414-420.

Zhang, C., and Moore, I. D. 1997. Finite element modelling of inelastic deformation of ductile polymers, *Geosynthetics international*, 4(2): 137-163.